8

Criterions for Selection of Volume Induction Heating Parameters

Niedbała Ryszard and Wesołowski Marcin
Warsaw Technical University
Warsaw, Poland

1. Introduction

Induction heating, with regard to a great number of applications in material processing, can be divided into two domains: surface and volumetric heating. In the first case, the criteria for parameters selection in induction heating installations are determined for skin depth and process time. In the case of volumetric heating, additional parameters, such as electrothermal efficiency and power control ability, must be taken into account. These requirements in connection with large variances of major electrical and thermal parameters of workpieces make the method multi-parameter and have a strong influence on high-frequency power sources. Without the knowledge of physical phenomenon and quantitative influence on temperature distribution it is unfulfillable to prepare a set of input data for effective modeling of the technological processes and directions for optimal selection of power sources.
Therefore the volumetric induction heating issues are a very complicated discipline that requires using of specialized calculating procedures for optimal selection of power sources for realizing an established technological processes. In this chapter some methods for modeling, designing and power controlling in volumetric induction heating systems were discussed.
In the chapter, the most popular methods for accurate power control in induction heating systems were analyzed in the case of nonlinearity material properties. Some examples were shown and classical approach for power control in the systems was compared to pulse width modulation case. The advantages and disadvantages of proposed construction and process solutions were discussed.

2. Volumetric heating – the basics

Volumetric induction heating is a very popular non-contact technology that has very wide applications in material processing. Operating frequencies are depended on the technology used. The spectrum ranges from low frequencies (50 Hz for heating a massive details), through the middle range (50 kHz for rafination and recasting processes) to high values (250 kHz and more for levitation melting etc.). Describing of all technologies as an universal problem is not possible, so in this chapter only selected topics were presented.
Induction heating modeling and simulation is a very popular domain, earlier by plurality of mathematical field and circuit models. Nowadays, there are numerous of numerical systems

that enable the simulation of complex coupled-physics electromagnetic and thermal problems. However, calculating systems usage often does not lead to practical applications solving, but to working out computational exercises. Analytical descriptions which used to be helpful in getting to know and making appraisals of electrothermal effects are being forgotten nowadays. Moreover, in the latest specialist literature concerning the issue of radio frequency induction heating, the electromagnetic part seems to be preferable. But it is worth to remember that basic knowledge on heating processes is essential to create input data that enable us to reaching our established targets quickly. An attempt to indicate the possibility of acquiring the first numerical approximation to the planned field decomposition has been undertaken on the example of inductive volumetrically heated charges. Not only material and geometrical properties of the charge but also extortive values- continually modified in the process of heating have the major impact on the way it is shaped. Therefore, cooperation of the source of power and inductive heating system is extremely important for the final result. The influence of dense electrical circuit parameters on the temperature field in the charge and vice versa is high enough to be taken under consideration. Moreover, simple relations arising from analytical models may determine the basis for an estimation of the quality of numerical calculations. Validated solutions to analytical equations may not only constitute the first approximation, but also explain physical basis of electrothermal effects in inductive heating much better.

When heated material is ferrous, material parameters are significantly important. Its main characteristics such as resistance and inductivity change during heating. A knowledge of the character of load changes enables to choose the right way of control. Defining the range of changes, including power (magnetic field strength on the surface of the charge) limits resonance frequency adjustment of the charge in magnetic state compared to the other states, including the final- nonmagnetic. It allows working out some more safe power adjustment algorithms in the frequency ranges which are being adapted.

Articles, in which electrothermal devices powered by real sources are being simulated, come out in the specialist literature exceptionally rarely. Attempts to verify results received are made even less often. It seems to be significantly important, when electric energy is being converted into heat in strongly nonlinear materials. Many comparisons show that simplifications assumed by many authors cannot provide useful results. Supplying of induction heating systems from high frequency energy sources is not optimally exploited. Generally energy sources are produced as current inverters. However, transistors frequency converters with voltage inverters can be recognized as very efficiency sources because of little self-losses. Unfortunately, nonlinearity of workpiece parameters can reduce efficiency of voltage sources by introducing additional inductances in high-frequency circuit.

2.1 Temperature distribution in heated bodies

In many cases the main goal of induction heating is to realize the heating processes with uniform temperature distribution within the heated body. This requirement is often hard to satisfy because of necessity to providing the maximum electrical efficiency of induction heating systems. In practice, the efficiency is increased by reducing process time and uniform energy consumption. Other important factors include maximum production rate, environmental friendliness and providing compact systems.

To display the temperature distribution within inductively heated body, a several analysis of long cylindrical bars were realized. The results were classified and carried to the average temperature of charge at the end of heating process. This average temperature was calculated according to equation:

$$t_{śr} = \frac{\sum_n V_n \cdot (t_n - t_0)}{V_C} + t_0 \quad (1)$$

Where: t_n - temperature of elementary volume V_n, V_c- total volume of charge, starting temperature, elementary thermal capacitance of charge assumed as constant.
All of the temperature deviations varying from the average value $\Delta t_n = t_n - t_{śr}$ are the same for charges of the same thermal efficiency η_c= *const* surrounded by a time-variable electromagnetic field that has the same relative frequencies. Relative frequencies were described as a proportion of a charge specific dimension (r_2) to the skin depth (δ_2): $\xi=r_2/\delta_2$. Another important factor, the elementary surface power p_F, which has a strong influence on the temperature uniformity, has been temporary neglected. According to the assumption which has been made earlier that the relation with the same radius of a charge is constant ($p_F \cdot r_2 = const$) (Rapport E. at al, 2006; Sajdak C. at al, 1985) proves that the omission of this parameter from designing has not influenced the final results. To show the results calculated for temperature distribution in inductively heated steel charge $p_F \cdot r_2 = 10\,\mathrm{W/m}$, some deviations from the average temperature $t_{śr}$=1100°C carried to the relative radius $rw=r/r_2$ were shown in figures 1 and 2. It has been proved that regardless of the heat loses (fig. 1) or of the heat sources distribution (fig. 2), all temperature curves were intersected into a common point located in the center of the charge volume (mass).
Results presented provides to modify the criterial temperature equation that applies in the case of heat conduction with arbitrary located heat sources (Zgraja J. at al, 2003).

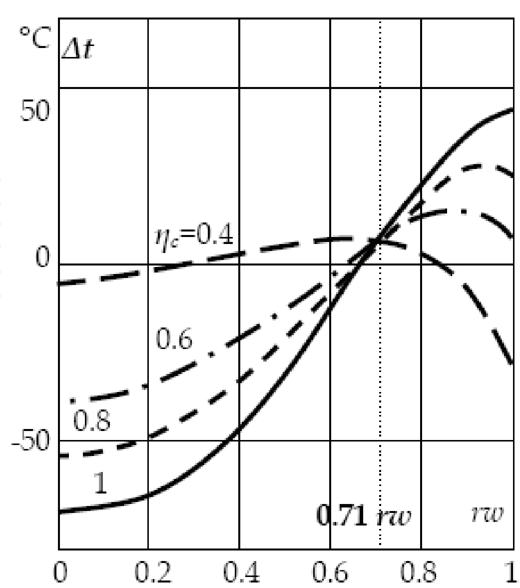

Fig. 1. Temperature divergences within inductively heated charges by frequencies of ξ=3, for different heat efficiencies

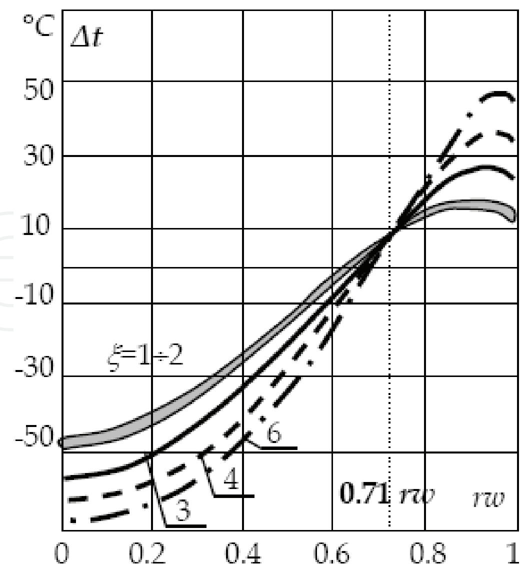

Fig. 2. Temperature divergences within inductively heated charges by different frequencies for constant heat efficiency η_c=0,8

$$K(\xi,\eta_c) = \frac{2\cdot\lambda\cdot\Delta t}{p_F\cdot r_2} = \eta_c\cdot\left[1-\frac{2.2}{\xi\cdot\sqrt{2}\cdot(\eta_c+1)}\cdot\frac{B(\xi)-1}{A(\xi)}\right] \quad (2)$$

Where:
λ - thermal conductivity, $B(\xi) = ber^2(\xi) + bei^2(\xi)$, $A(\xi) = ber(\xi)\cdot ber'(\xi) + bei(\xi)\cdot bei'(\xi)$.
In the equation presented above momentary heat efficiency (as the proportion of stored power and dissipate power of charge) and total heat efficiency were determined as a linear approximation in time domain, calculated as $0,5\cdot(\eta_c+1)$.
On the other hand, maximal temperature divergences Δt_{max} in a cross-section of the charge were calculated. The divergences refer to $\Delta t = (p_F\cdot r_2)/(2\cdot\lambda)$ that enable us to calculate the criterial temperature $K_{\xi\eta c}$ based on field analysis. The comparison of numerical and analytical results has been presented in the figure 3. The convergence between calculating results was very high for both cases of all frequency ranges (fig. 3a) and heat efficiency (fig 3b) practical spectrum. All results were compared within the same, constant material properties. This simplification does not result in significant errors at the end of volumetric heating process.
Additional verification of K coefficient has been accomplished by determining maximal temperature differences (calculated by using equation no 2) and using forward calculations shown in figures 1 and 2.
The results has been presented in figure 4. The convergence between analytical and numerical calculation results have reached a high value. Main difference was that the extreme value of the temperature was not located in the external surface of the charge.

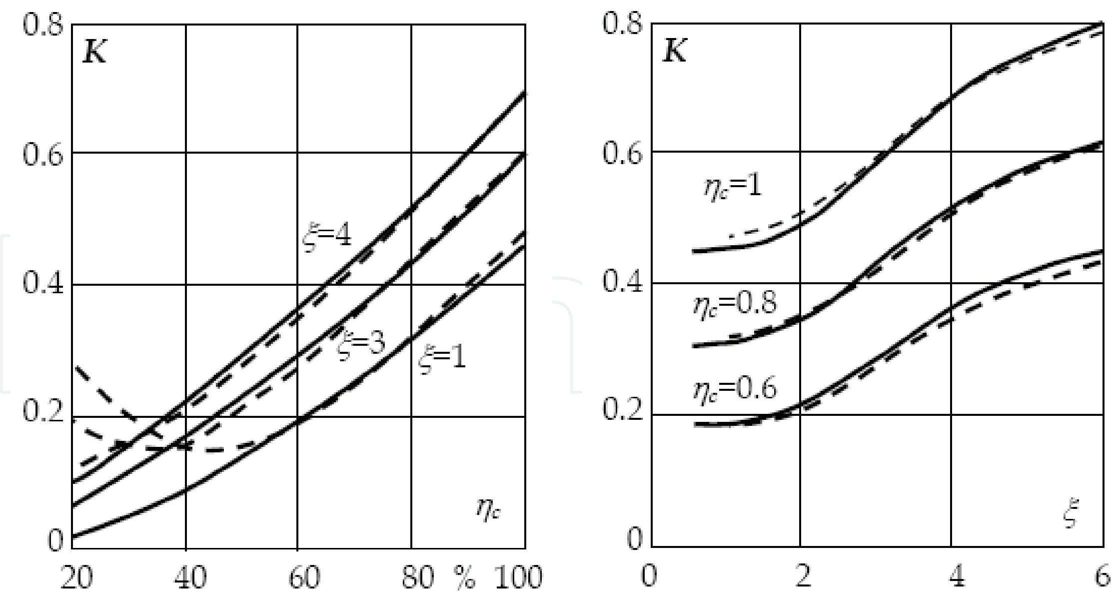

(a) (b)

Fig. 3. Criterial temperature values from analytical (solid lines) and numerical (dash lines) calculations as a function of heat efficiency η_c (a) and relative coordinate ξ (b)

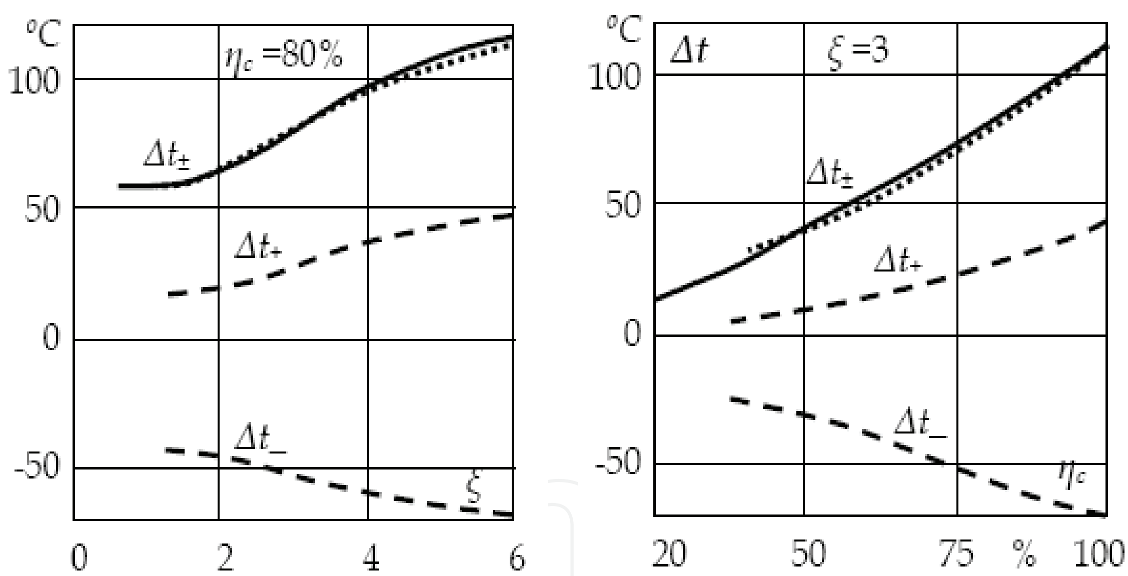

(a) (b)

Fig. 4. Positive Δt_+, negative $\Delta t\_$ and summary $\Delta t_\pm$ temperature differences in cross-section from numerical (dash lines) and analytical (solid lines) analysis as a functions of heat efficiency η_c (a) and relative coordinate ξ (b)

2.2 Time and energy in induction heating process

The design criteria for induction mass heating systems which seems to be the requirement for temperature uniformity of the charges is only one of the goals. Another important factor includes minimum process time and energy consumption. Heating time (fig. 5) is determined by the temperature differences in charges cross-section, frequency and heat

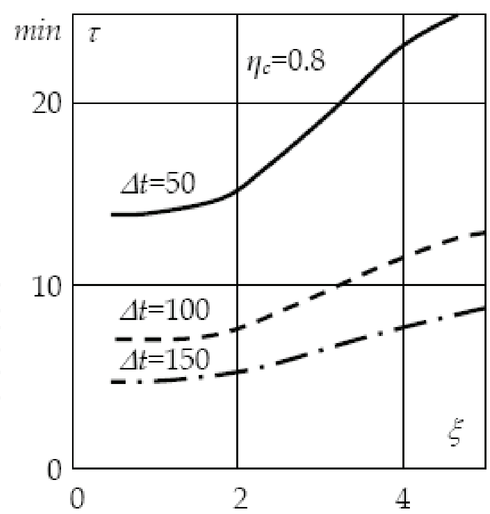

Fig. 5. Exemplary heating times calculated for workpiece of outer radius r_2=0,05 as a function of ξ, for different temperature uniformities

efficiency. Additional, this parameter is a function of radius of workpieces and can be determined by the following equation:

$$\tau(r_2, \Delta t, \xi, \eta_c) = \frac{q_a \cdot r_2^2 \cdot K(\xi, \eta_c)}{2 \cdot \Delta t \cdot \lambda \cdot (\eta_c + 1)} \tag{3}$$

Where: $q_a = \gamma_{śr} \cdot c_{śr} \cdot (t_{śr} - t_0)$ - elementary heat capacity of charge
The elementary electrical energy consumption is determined only by the efficiency of heating system, without taking into consideration the temperature uniformity requirement:

$$e(\xi, \eta_c, m, r) = \frac{2 \cdot c_{śr}}{(\eta_c + 1) \cdot \eta_e(\xi, m, r)} \tag{4}$$

Where: $c_{śr}$ - average specific heat, $m = \sqrt{\frac{\rho_2 \cdot \mu_2}{\rho_1 \cdot \mu_1}}$, $r = \frac{r_1}{r_2}$ - proportion of material properties and radiuses of inductor and workpiece.
The energy consumption rate for steel heating has been presented in figure 6. The model of long cylindrical bar of the radius r=1,4 was used.
The criteria for heating time and energy consumption minimizing cannot be satisfied by optimization of process frequency. Optimal frequency range for exact process has to be described using criterion criteria of minimal time which is limited by the temperature uniformity and type of power source.

2.3 Circuit parameters of induction heating system

Due to the assumption that value of relative coordinate $\xi = r_2/\delta_2$ is dependent on the frequency, the only independent property from the workpiece geometry is absolute heating power. The maximum value of the power can be determined by equation 5.

$$Pc(\Delta t, \xi, \eta_c, m, r) = \frac{4 \cdot \pi \cdot \lambda \cdot \Delta t}{K(\xi, \eta_c) \cdot \eta e(\xi_2, m, r)} \tag{5}$$

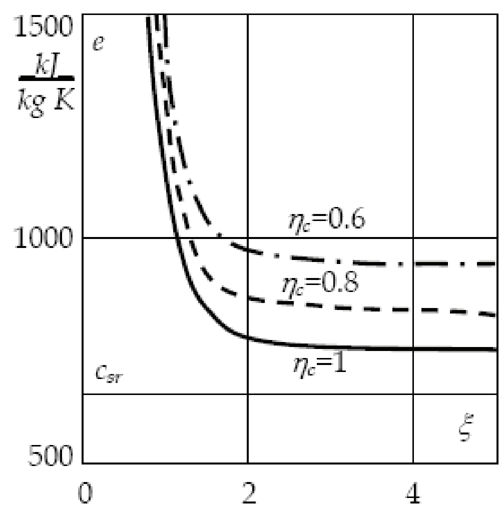

Fig. 6. Elementary electric energy consumption as a function of ξ, for different heat efficiencies

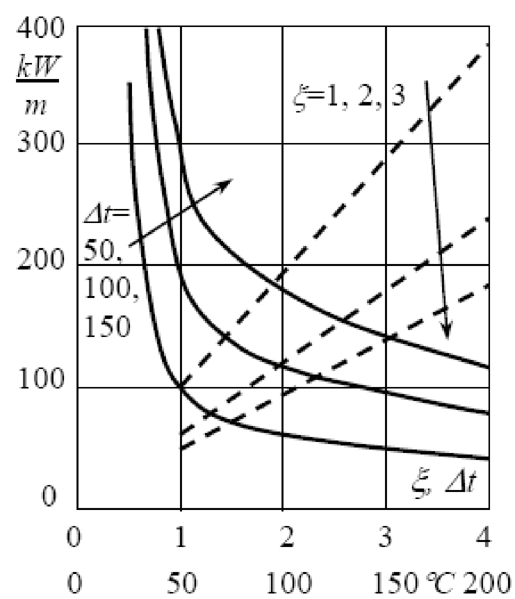

Fig. 7. Maximal power values of induction heating system for the case of heating the steel cylindrical bar (r=1.4) as a function of ξ i Δt.

Power values have been shown in the figure 7. The values can be used to determine the total source power or current linkage $I \cdot n = H_0$.

$$H_0(\Delta t, \xi, \eta_c) = \sqrt{\frac{2 \cdot \lambda \cdot \Delta t}{\rho_2 \cdot \xi \cdot \Phi r(\xi) \cdot K(\xi, \eta_c)}} \tag{6}$$

Current linkage or magnetic field intensity, depending on the power source type, are highly variable by the heating time. These variables should be corrected basing on momentary value of system impedance, especially in induction mass heating systems, where the variable of system parameters can reach a high values. The range of impedance in steady state can be determined by using the method of equivalent resistances, which are independent from workpiece geometry:

$$R_2(t,H) = 2 \cdot \pi \cdot \rho_2(t) \cdot \xi(t,H) \cdot \Phi r(t,H)$$

$$X_2(t,H) = R_2(t,H) \cdot \frac{\Phi x(t,H)}{\Phi r(t,H)} \tag{7}$$

Equivalent resistances, supplied by workpiece resistance and inductive leakage reactance (8) can be used for determination of impedance variance from material properties (9)

$$R_1 = \frac{R_2(t,H) \cdot r}{\Phi r(t,H)} \sqrt{\frac{\rho_1}{\rho_2(t) \cdot \mu_2(H)}} \quad X_0 = R_2(t,H) \cdot \frac{\xi(t,H)}{\Phi r(t,H)} \cdot (r^2 - 1) \tag{8}$$

$$Z(t,H) = R_2(t,H) \sqrt{\left[(1 + \frac{r}{\Phi r(t,H)} \sqrt{\frac{\rho_1}{\rho_2(t) \cdot \mu_2(H)}}\right]^2 + \left[\frac{\Phi x(t,H) + \xi(t,H)(r^2 - 1)}{\Phi r(t,H)}\right]^2} \tag{9}$$

Impedance shown above or its resistance and reactance enable for determinate the induction system parameters. Power values in specific time intervals of heating process for the cases of current source (10a), power source (10b) and voltage source (10c)

$$Pc(t,H) = (I \cdot n)^2 \cdot \frac{R_2(t,H)}{\eta_e(t,H)} \tag{10a}$$

$$Pc(t,H) = Pc \tag{10b}$$

$$Pc(t,H) = \left(\frac{U}{n}\right)^2 \cdot \frac{\cos\varphi(t,H)}{Z(t,H)} \tag{10c}$$

3. Ferrous bodies heating

Material properties have a strong influence on induction heating process, especially in cases of ferrous materials. Resistance and reactance of charges are strongly variable in heating time. The parameters range should be taken into consideration for proper selection of power source and control systems. Determination of the range of resistance and reactance variances and also minimal value of momentary power (magnetic field intensity in the workpiece surface) reduce the range of resonant frequency at the beginning of process (in magnetic state) from other states (non- magnetic at the end of heating process). Determination of the power (from equation 10) values for different states, for example for low temperature range, for Curie point and at the end of the process, can be used for planning the heating process with extremely electromagnetic and thermal values. Such calculations enables users to design safety algorithms for precisely power controlling in frequency domain.

Analysis of energetic relations in induction heating system was based on example of the system supplied from voltage source. Let us assume the workpiece of outer radius r_2=0,05 m, placed in high-intensity electromagnetic field. The air gap between workpiece and inductor was extremely short (r=1,1) to underline variable of workpiece parameters influence on the instantaneous absorbed power. The heating process was very dynamic,

such in the figure 8. The marked area in this figure was used to illustrate the time range of two states (magnetic and non- magnetic).
In the figure 9 the results of static characteristics comparison was shown. Except from low temperatures and Curie temperature, even simply linear characteristic (parameters for high temperatures) is characterized by quite convergence to real process.

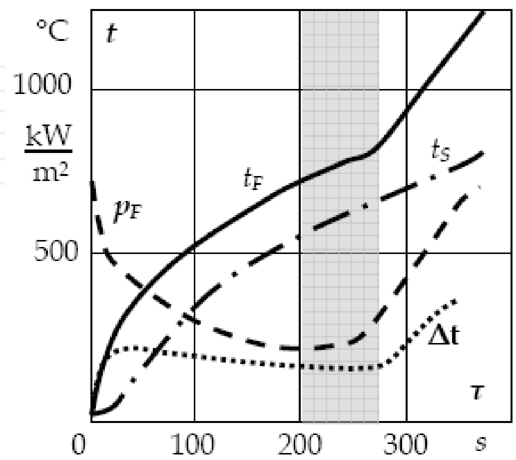

Fig. 8. Time characteristics of temperature and surface power for the case of voltage source: t_F - temperature of external surface of workpiece, t_S - temperature in the centre of workpiece, p_F - surface power

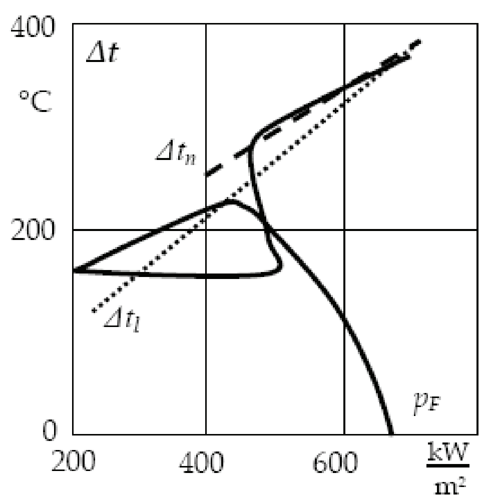

Fig. 9. Numerical and analytical static characteristics comparison $\Delta t=f(p_F)$ for the case of voltage source. Solid line- field calculations; dash and dot lines- analytical calculations Δt_l - linear, Δt_n - nonlinear

4. Accuracy of numerical modeling of induction heating systems

Modeling of induction heating systems seems to be the well-known and often used discipline. There is a lot of commercial and non- commercial calculating systems (for example FEM systems) that enable users to solve such problems automatically. The numerical system used different types of techniques for solving coupled – field problems. In present time, many authors (Galunin S. at al, 2006; Paya B. et al., 2002) describes a very advanced numerical models and take into consideration many of physical phenomenon like multiply reflection effect in radiation heat transfer or phase changes. This approach complicates models and prevent them from having the ability of calculations verification. There is a less information about accuracy of numerical modeling of coupled problems. This fact essentially limits the utility of numerical calculations in practical applications. In this chapter the numerical modeling and simulation accuracy problems were taken into account. Some popular MES calculating systems were used and simulation results were compared to the analytical ones and measurement results of physical model. In the first case, the induction heating system shown in figure 10 was used. The dimensions and properties of the model were the same like in the previous chapters. Nonferrous long cylindrical bar was used as the workpiece during simulations. Outer diameter of the charge was 24 mm. Air gap between worpiece and inductor were minimized (1 mm). Some of the basic material properties of charge – inductor system were shown in table 1.

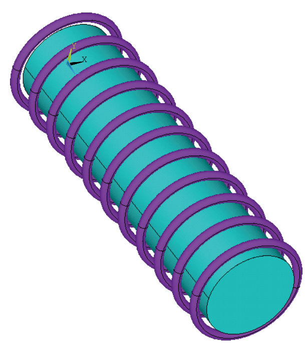

Fig. 10. Geometry of model

	μ_w -	ρ $\Omega \cdot m$	λ $W/(mK)$	c_w $J/(kgK)$	γ kg/m^3
Workpiece	1	$3{,}8 \cdot 10^{-7}$	12	654	7800
Charge	1	$1{,}78 \cdot 10^{-8}$	200	380	8933

Table 1. Material properties of the model

During modeling process the two - dimensional axisymmetric numerical models were used. The task has been solved analytically at first. The power consumption rate was used for the energy equation determination as well as for determination of basic parameters of induction heating system. Calculated parameters were used as an input data for numerical calculations. The final results of such calculation were temperature characteristics of thermal analysis of the induction heating problem. Numerical calculations were made by using the coupled – field analysis of electromagnetic field (harmonic problem) and thermal field (transient heat transfer problem). Such approach was necessary in view of different time constants for analyzed fields.

At first, some results of analytically and numerically calculated magnetic field intensity were compared. Two cases were compared for different sources of energy: the impressed current source (500 A) and equivalent current density source. The basic goal of the comparison was to calculate the errors rate by assuming simplification of using current density source instead of the general voltage or current source. The numerical results were compared to analytical ones and radial distribution of magnetic field intensities was shown in figure 11.

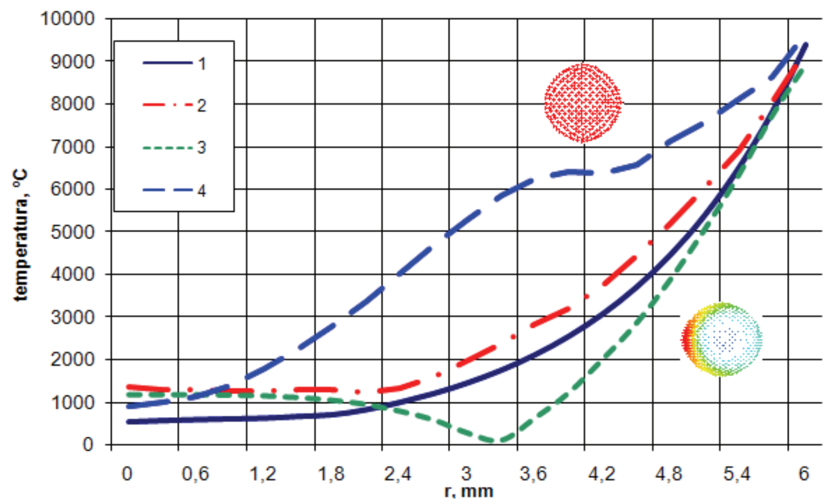

Fig. 11. Radial distribution of magnetic field intensity: 1 - ANSYS results for current source; 2 - ANSYS results for current density source; 3 - Quick Field results for current source; 4 - Analytical results

The results shown in figure 11 proves some huge differences, as quantitative as qualitative in magnetic field distribution within the workpiece calculated by using both analytical and numerical methods. Relative insignificant differences from analytical solution were obtained by using the Quick Field program. Simulation results from ANSYS in the case of current source were characterized by errors level reached 50% from analytical results. However, maximal errors were received in ANSYS in the case of current density source. For numerical results errors values were calculated for skin depth and shown in the figure 12.

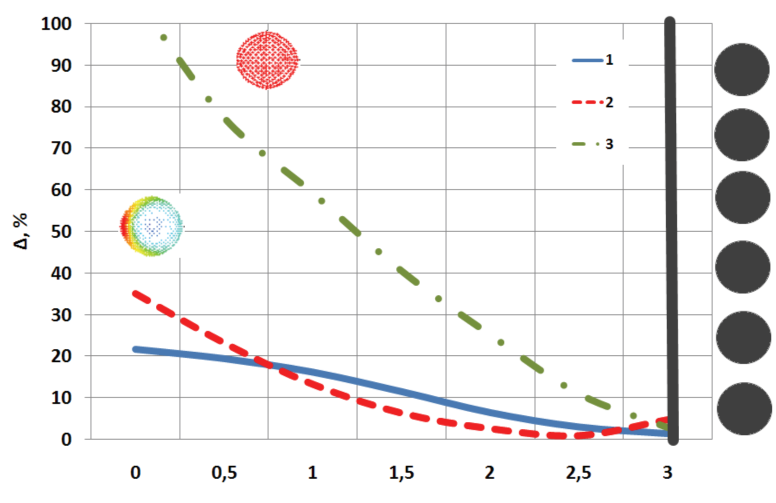

Fig. 12. Magnetic field intensity differences between analytical and numerical simulation results for the cases of current source (1) and equivalent current density source (2) in ANSYS system and current source in QF system(3)

The results presented above shows that in such heating systems the proximity effect determinates current conduction conditions in the workpiece. This rule is especially

important in high efficiency induction heating systems, where dimmensions of air gap between workpiece and the inductor should be as minor as possible. In systems of large dimmensions of the air gap, the proximity effect is less important and establishment of refered simplification can affor much less calculation errors.
Basing on simulation results of magnetic field energy, the heat source distribution (Joule heat generation) in the workpiece was calculated and used in heat transfer analysis. In view of differences between results, both as a funcion of radius and heigh of workpiece, thermal analysis was solved by using of most accuracy results. Transient heat transfer phenomenon was solved by heating time 600 s. Boundary conditions were the same like in the analytical solution. The problem was solved in two different FEM systems (QF and ANSYS). Three algorithms were used for solving the coupled field problems. The simulation results were used to compare both methods and calculate a global accuracy of numerical simulation of induction heating phenomenon. Heating characteristics were shown in the figure 13.
It is noteworthy that simulation results of induction heating process as well as in ANSYS and QF systems are significantly different and slightly compared to conventional methods. Maximal differences between the results has reached the value of 170 K. Additionally numerical results are not compared to analytical ones. The differences from assumed temperature has reached 80 K for both ANSYS and QF results. Even simulation results from equivalent (Physical environment and MFS) solvers were significantly different in the evaluation of dynamics temperature characteristics and temperature chart after 600 s of heating.

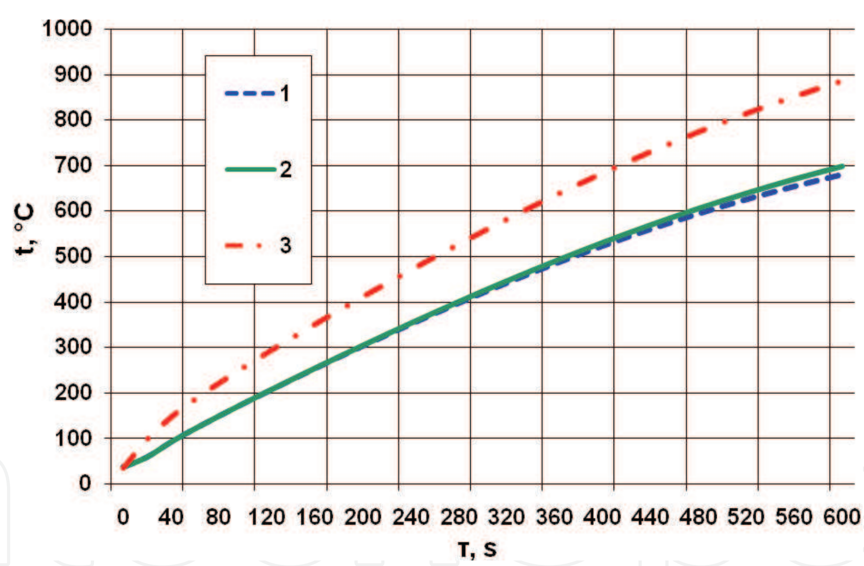

Fig. 13. Calculated temperature evolution curves at the longitudal center of bar: 1 - ANSYS physical environment results; 2 - ANSYS MFS results; 3 - QF results

The simulation results of magnetic field distribution show a significant differences between analyzed case depended of many factors, such as the manner of assuming power source in inductor, discretization rate or solver used during simulation process. This study has shown the disadvantages of the coupled field modeling with analytical approach. The calculated results of magnetic field intensity and current densities were two times different. The differences reached during the simulation process enable us to affirm the low usefulness of numerical simulation in practical problems and quantitative simulation of induction heating process.

There is a small number of articles and references, where the problems of induction heating systems were analyzed, and where the real power sources have been taken into account as well. Additionally, it is not many reliable verifications of numerical simulations with real processes. These results are significantly important when electrical properties are slightly dependent on the temperature. Many of verifications of experimental validations with the computed ones provides the influence of numerical models simplification onto results. The simplifications can afford the low practical usefulness results. As an example the authors of the article (Paya B. et al., 2002) presents the results of a series of tests made in order to validate the magneto – thermal module of the FLUX3D system. The physical model used for studying the induction heating was a cylindrical tube of magnetic steel, external diameter 100 mm, thickness 5 mm, length 300 mm. The inductor has been supplied by thyristor inverter working at 2,75 kHz. Figure 14 presents the comparison of the model and the experiment of the evolution of temperature at certain point at outer surface. It shows a huge differences between the model and experiment, especially in the case of ferrous materials heating.
This study has shown the advantages and the drawbacks of the coupling way compared to the linking way. The linking way may be profitable when the electrical properties are slightly dependent on the temperature because the computation time is strongly reduced. Otherwise, for example, when reached Curie temperature, the coupling way is the only one which can provide acceptable results. According to the experiment, it is also necessary to put more accurate physical properties at different temperatures to describe the behavior of the material correctly.

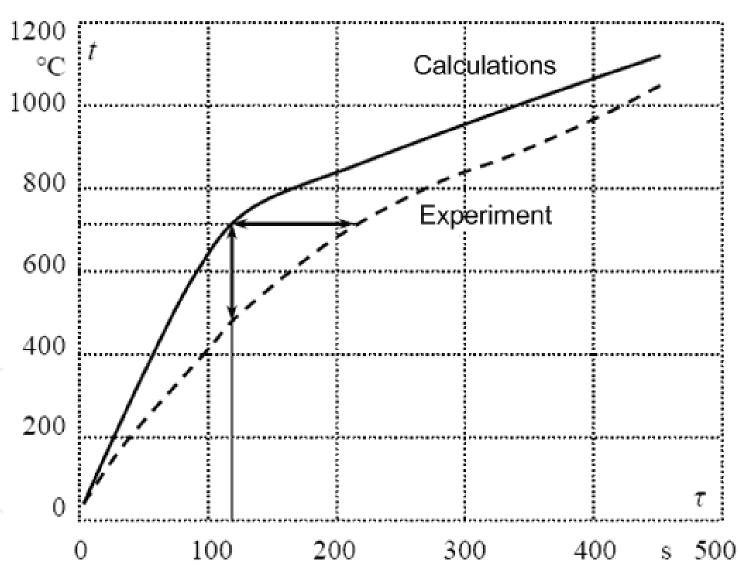

Fig. 14. Comparison of the experimental results and the computed ones (Paya B. et al., 2002)

5. Frequency inverters in induction heating systems

Basic calculations of induction heating systems in most cases takes into consideration only the workpiece – inductor system. There is a small number of articles, where electro-thermal converters were simulated and fed from the real power sources. Supplying the induction heating systems by energy sources based on the topology of frequency converters cannot be fully exploited. In many cases current source inverters have been used. In spite of minimal

power losses of transistor frequency inverters, the variable workpiece properties make the cooperation with heating system difficulty. Properties of such sources can afford some complications in control system and reduce the system efficiency (generator and heating system) by inserting an excessive inductances to the system.
Such power sources are commonly used for melting of precious metals, continuous heating of sheets (ribbons, wires), remelting, refinement, tempering and other processes when the properties are slightly dependent on temperature. On other hand, in processes like steel heating, hardering etc (when impedance are highly dependent on temperature), utility of such sources is highly limited and application of complex control algorithms is required. In many cases, to avoid this requirement, maximal internal inductances and multi-layer inductors are being exploited. Increasing inductance stabilizes the charge variables but decreasing the system efficiency. In many articles the advantages of frequency converters are emphasized. But there is not many analysis about using converters in specific technologies.
Disregarding from power and high frequency ranges, the number of thermal application of heating materials in multi geometry inductors is wide enough. Induction heating can be divided into two domains: surface and volumetric heating, but based on conditions for selection of power source, into huge and low scattering systems. The scattering rate depends on air gap reactance and additional reactance of system chokes. The scattering effect do not have any influence on induction heating system efficiency (11) (Rudnev V., 2003)

$$\eta e(f,t,H,Dd)=\frac{1}{1+\sqrt{\frac{\rho_w}{\rho(t)\cdot\mu(H)}\cdot\frac{Dd}{\phi[f,\rho(t),\mu(H)]}}} \tag{11}$$

Where: f - frequency, t - temperature, $\rho(t)$ - workpiece resistivity, H - magnetic field intensity, $\mu(H)$ - magnetic permeability, ρ_w - inductor resistivity (based on workpiece resistivity), Dd - geometry of heating system, ϕ - shape coefficient.
Scattering effect have a strongly influence on heating efficiency of the workpiece (12).

$$\eta c(f,t,H,Dd,t_F)=1-\frac{P_{SC}(t_F,Dd)}{P2[f,\rho(t),\mu(H),\rho_w,Dd]} \tag{12}$$

Together with increasing frequency, the voltage on air gap increases and power rate dissipates in the charge (*P2*) decreases. Basing on references, maximal value of heat loses (*Psc*) depends only on geometry and on the type of insulating material, without taking into consideration the kind of power supply system (Haimbaugh R. E., 2001; Rudnev V., 2003; Rapoport E. at al, 2006) . The power system influence is not practically determined in respect of necessity of coupling the field (inductor – workpiece) and the circuit (power supply – load) analysis. Such analysis is a very time-consuming process. Additionally a special calculating procedures should be used and a variance of dynamic impedance during heating process must be taken into account.
The indicator of energy conversion quality is electro – thermal efficiency of induction heating system. In all time steps, for the workpiece of known properties can be calculated from equation (13).

$$\eta et(f,t,H,Dd,t_F)=\eta e(f,t,H,Dd)\cdot\eta c(f,t,H,Dd,t_F) \tag{13}$$

Circuit parameters of induction heating system were calculated basing on approximate method of equivalent resistances (Rudnev V., 2003). Load parameters and voltage source model were used for induction heater parameters determination. The physical model used for studying a induction heating was a ferrous steel cylindrical bar of external diameter d = 12 mm , surrounded by a 7 turns coil, internal diameter 22 mm, length 31 mm. The series capacitor was selected in manner that frequency in high temperatures (at the end of the process) satisfied the volumetric heating requirements (Rudnev V., 2003). The operating frequency was at f_g=30 kHz. The system was supplied by a step-down transformer (transfer ratio 40:1) by the voltage inverter. In the figure 15 some efficiency characteristics in frequency domain has been shown. The electric efficiency for analyzed case was constant in practice (dash line in fig. 15). So that, only thermal efficiency determinates the rate of total electro – thermal efficiency. If the value is smaller, the maximal value of efficiency curve has reached a lower value of frequency.
Characteristics presented in the figure 15 were determined for nonferrous charge for one time step. The momentary values of maximal efficiencies during heating the steel charge has been shown in figure 16. Additionally, the changes of power coefficient were shown.

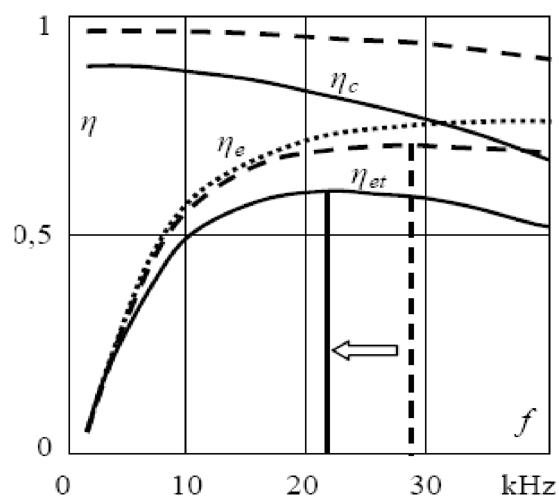

Fig. 15. Efficiencies of induction heating system as a function of frequency

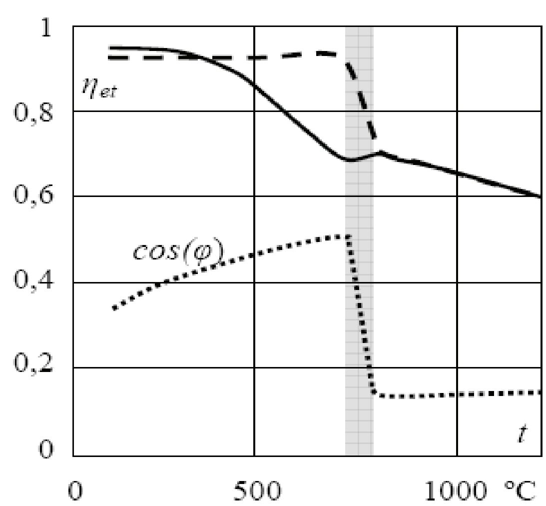

Fig. 16. Efficiency of heating process and the power coefficient in function of workpiece temperature

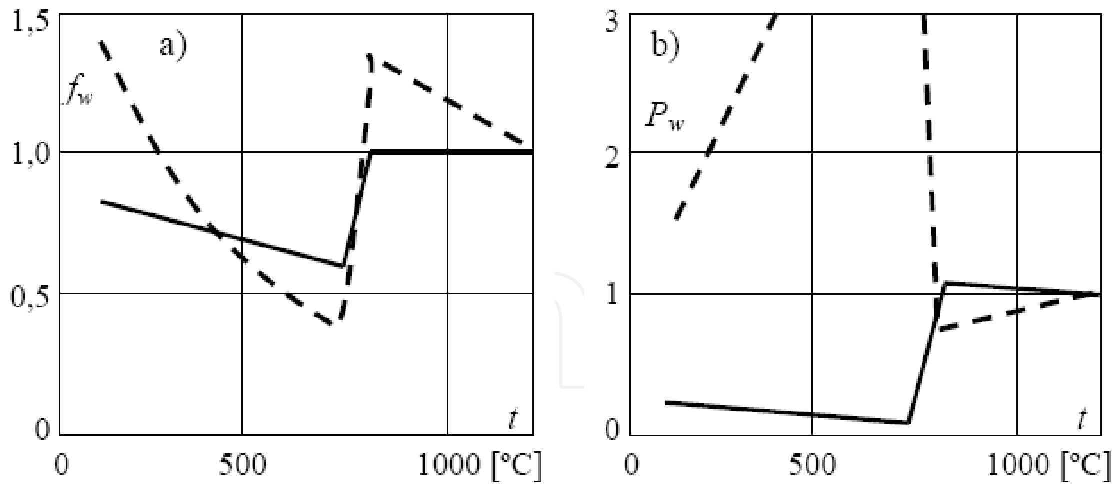

Fig. 17. Relative variances of chosen parameters of induction heater for maximal value of efficiency during all process time: a) – frequency with reference to the end process value (30 kHz), b) - active power with reference to the end process power (2600 W). Before (dash line) and after (solid line) reactive power compensation

In the next step, the heating process in two cases was analyzed: with (solid lines in figure 17) and without (dash lines in figure 17) the series capacitor. The value of capacitor was determined by satisfying the requirement for reactive power compensation at the end of the heating process. Comparison of such heating processes have been made for the case with and without the capacitor. In second case, the source voltage on inductor was pulling up to the specific value, when active power in the charge has reached the same value as in the compensation process. Non-compensating inductor voltage is larger: $Q = \omega \cdot L/R$. To provide the maximal efficiency values during the whole process, the frequency range should be changing. The frequency changes, carried to the end of the process has been shown in figure 17.a. The active power curves during the heating process were shown in figure 17.b.

The series capacitor variant, the resonant voltage inverter, minimizes the range of characteristics values variances. The case was characterized by better, corresponding to heat losses, power profile, that produces isothermal heating process.

6. Voltage frequency inverters

In induction heating systems of medium frequency range, both thyristors and transistors inverters are used as an power suppliers (Haimbaugh R. E., 2001). Voltage supply systems are commonly configured as the bridge systems. Voltage source inverters are not often used for direct supplying of the induction heating systems. The reason of such practice is complicated control ability, especially in the cases of ferrous materials. In such systems, the current source inverters are commonly used. The inverters are characterized by simplicity of process realizing but their energetic efficiencies are significantly smaller.

Thyristors and transistors inverters, except from operating frequency ranges, are characterized by the different operating frequency changes during the heating processes. The thyristors should work with frequencies smaller then resonant ones. Different characteristics describes transistor circuits, which are characterized by large operating frequency range. The power sources based on transistors are better for feeding an universal induction heating systems.

a) b)

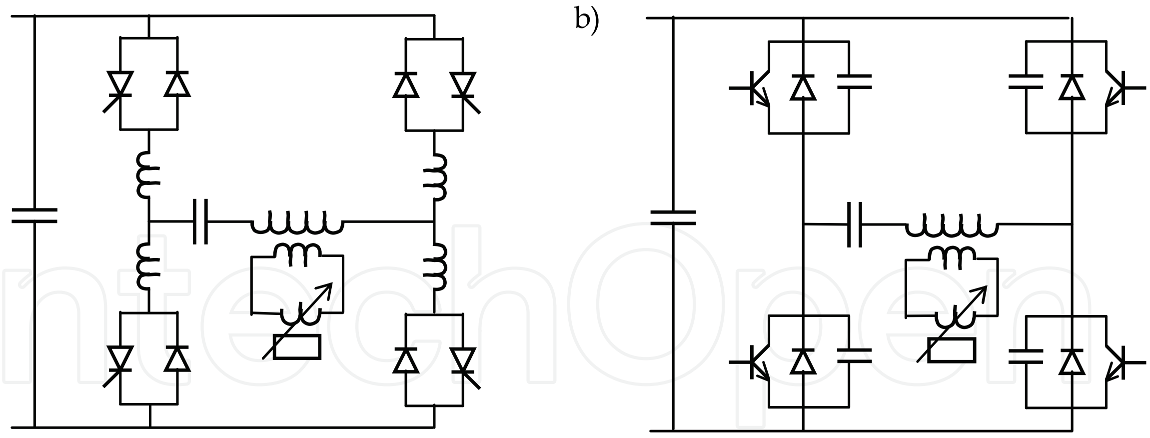

Fig. 18. Frequency inverters for induction heating systems: a) thyristors inverters $f < f_0$;
b) transistor inverters $f > f_0$

Some of the new innovative manners for inverters system control (fig. 18) can provide more useful and better operating characteristics in induction heating systems. The datasheets focusing on developed transistor generators are limited in most of the cases just to revealing basic information (Rudnev V., 2003; Rapoport E. at al, 2006) about frequency range, maximal output power and range of power regulation, efficiency, etc. Information about power and frequency adjustment ability to realized processes or inductors parameters are not frequently published. Lack of the basic data makes it difficult to precisely design the energetic save processes.

Transistor inverters are characterized by the ability to control frequency, voltage and pulse width modulation. In the model described previously, some calculations have been done using different types of commonly used power control systems of induction heaters:

- voltage;
- frequency;
- pulse width modulation.

7. Power control systems

Power control during the induction heating process seems to be basic factor for precise realization of the temperature uniformity requirement. Maximal value of the power in analyzed heating system was determined by following parameters of power source:

constant voltage U_0=300 V, resonant frequency f_g=30kHz and the constant duty factor w=1.

Three different analysis have been solved for momentary power ranges as a functions of feeding voltage, frequency and a duty factor. The curves of relative variances of power p_g, p_z were shown in the figure 19. The results shown in the following figure are presented as the functions of the relative variables (14) described as the proportions of momentary values of voltage, frequency and duty factor to the characteristic values described above.

$$x = \frac{U_i}{U_0},\ \frac{f_i}{f_0},\ \frac{w_i}{1} \tag{14}$$

Presented results shows the phenomenon that for significant frequency increase, the dissipated Power decreases rapidly. Changes of the duty factor enables to linear power controlling. In this kind of power control system, the insignificant increase (for the high temperatures range) or decrease (for the low temperatures range) of operating frequency is necessary. This phenomenon was shown in figure 19 (dash line *fw*). Constant value of frequency can be supported only in the case of voltage control for nonferrous material. In the case of ferrous materials, the heating efficiency increases strongly for less power values. In the figure 20 the phenomenon of efficiency increase for ferrous and constant values for nonferrous have been shown for three analyzed control systems.

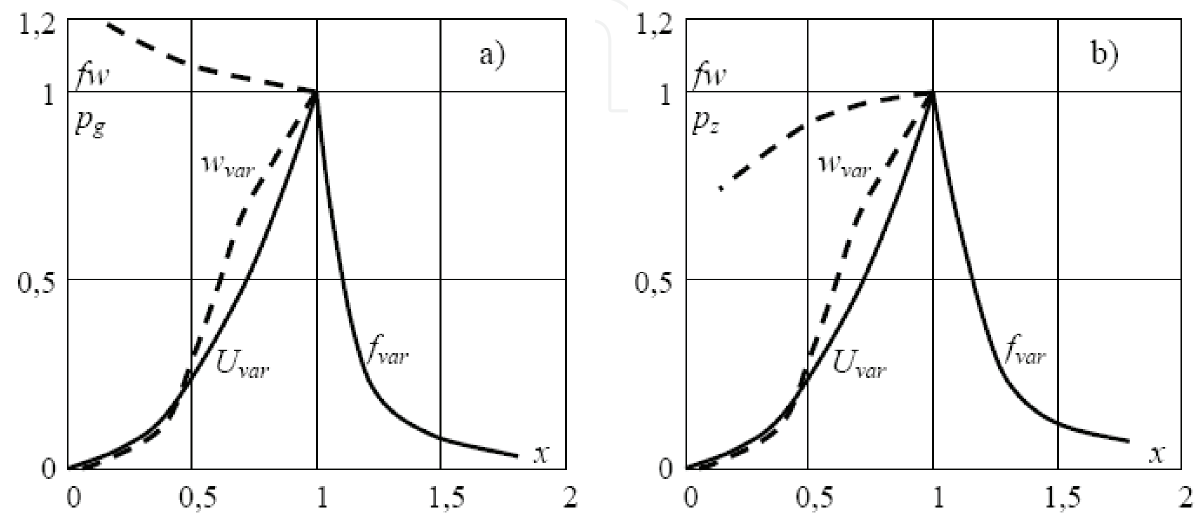

Fig. 19. Power control of the heater: voltage U_{var}, frequency f_{var}, duty factor w_{var} with variables *fw*, a) nonferrous charge, b) ferrous charge.

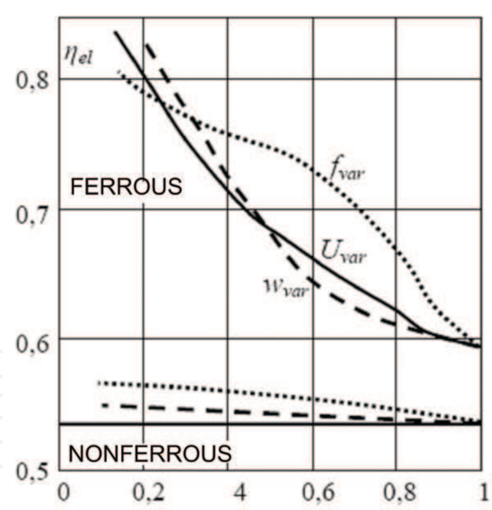

Fig. 20. System efficiency in function of variable set values for the case of ferrous and nonferrous charge

7.1 PWM controls system

Classical approach for power control of induction heating systems by frequency or intermediate voltage regulation is commonly used, well-known domain. For the case of voltage duty factors controllers, operating characteristics should be additionally discussed. Without instantaneous phase control (moment of transistors firing), the switches triggers at the moment of voltage wave synchronizing with maximal value of inductor current. The phenomenon has been shown in the figure 21. In this case, for frequencies near resonant, the current waveform is quite similar to sinusoidal one. The current wave deformation can be observed only for low pulse duty factors. In the figure 21 the inductors current (dot line) with its first harmonic (solid line) were compared for the pulse duty factor *w*=0,1 .

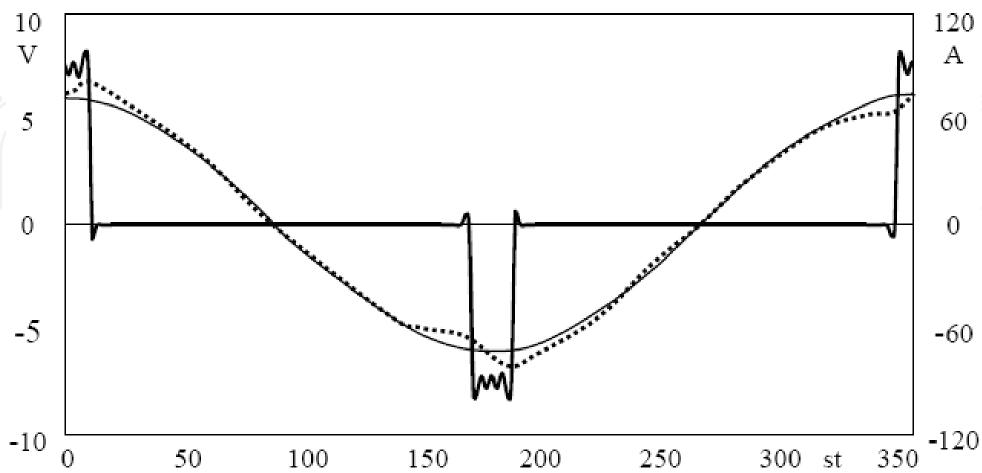

Fig. 21. Voltage and current waveforms for basic pulse duty factor controlling.

This manner for PWM control have some faults. Basic hazard is ability to decrease adjustment frequency below the resonance. Transistors can be destroyed in this condition. Other ability is forced controlling of the moment of transistors firing. This manner is quite better and can provide a lower current wave deformation. The case of transistors firing at the moment of current wave polarity change have been shown in figure 22.

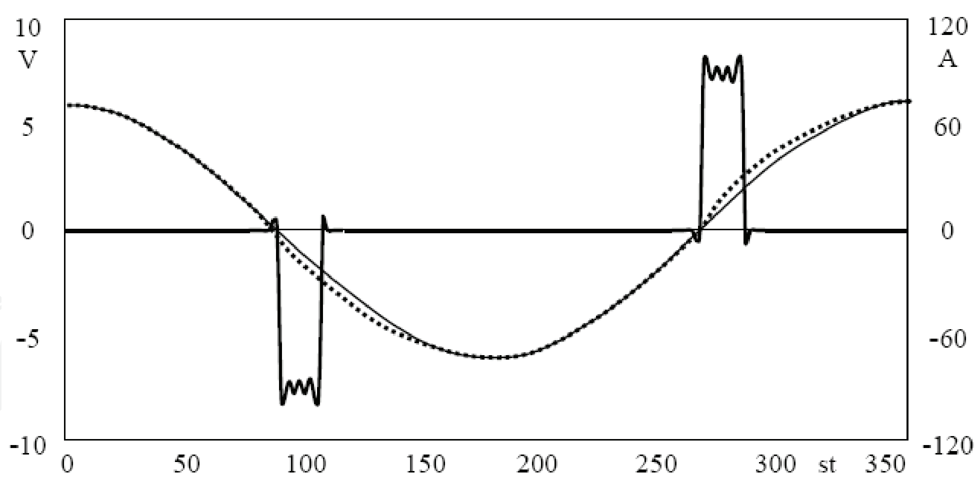

Fig. 22. Voltage and current waveforms for forced pulse duty factor controlling

Controlling of voltage impulse generating can provide the ability of keeping load characteristic of induction heater generator as an resistive or inductive-resistive during the process. Advanced transistors firing (from current wave) can be used for saturating power control in the system. The phenomenon of such approach is from that in this case two power control manners were used: the pulse width modulation of voltage and frequency modulation. In optimal operating conditions of generator (near resonance frequency) the changes of active power values as a function of inductors current can be observed. The characteristics presented in figure 23 shows the phenomenon. The shape of the curves is quite similar to the case of resistance furnace controlled by thyristors.

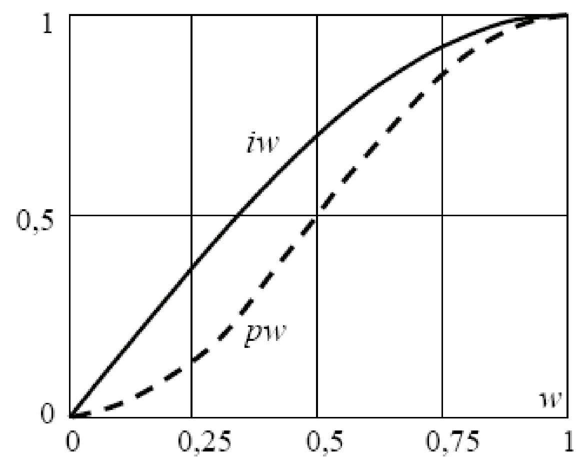

Fig. 23. Inductors current and active power of generator as a function of PWM value

7.2 Simulation results

Simulation of voltage and current waveforms and power control methods as a result were solved by using the harmonics method. The equation of voltage waveform was written as:

$$U_\tau = \sum_k u_{k,\tau} \tag{15}$$

Where all of harmonics depends from amplitude U_0, time (frequency) $\tau\,(\omega)$ and duty factor w:

$$u_{k,\tau} = \frac{4 \cdot U_0}{\pi \cdot (2 \cdot k - 1)} \cdot sin[(2 \cdot k - 1) \cdot \pi \cdot w] \cdot cos[(2 \cdot k - 1) \cdot \omega \cdot \tau] \tag{16}$$

Based on previous equation, the ability of power control range can be estimated. For studying a control systems *k=1...40* of odd harmonics were used. The impedance of heating generator was calculated by using the equivalent resistances method and particular current harmonics were calculated for different temperature values:

$$i_{k,\tau,s} == \frac{4 \cdot U_0}{\pi \cdot (2 \cdot k - 1) \cdot Z_{k,s}} \cdot sin[(2 \cdot k - 1) \cdot \pi \cdot w] \cdot cos[(2 \cdot k - 1) \cdot \omega \cdot \tau - \varphi_{k,s}] \tag{17}$$

Current in the series branch of generator was determined as the consequence.

$$I_{k,s} = \sum_k i_{k,\tau,s} \tag{18}$$

The simulation results for chosen steady state has been show in the figure 24. Voltage waveforms of PWM control system and the equal current waveform were depicted. In this kind of power control system, increasing of the operating frequency is necessary as described in previous chapter. Frequency increasing additionally provides to decreasing of momentary power value. So that it has been proved that controlled power value decreases faster than pulse width.

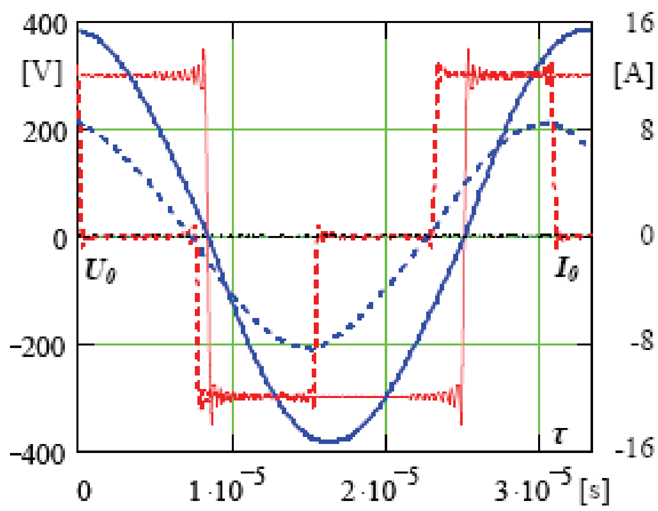

Fig. 24. Voltage and current waveforms in voltage inverter without the power control (solid lines) and for the case of PWM (dot lines) system

8. Conclusions

This chapter describes very widely the issues of the volume induction heating phenomenon. The criterions for selection optimal parameters of the induction heaters were discussed. It has been proved that in the case of volumetric heating, additional parameters, like electrothermal efficiency and power control ability must be taken into account to satisfy all requirements for optimal process implementation. Without the knowledge of physical phenomenons and quantitative influence on temperature distribution it is unfulfillable to prepare a set of input data for effective modeling of the technological processes and directions for optimally selection of power sources.

Basics rules of induction mass heating were described at first. Classical and modern calculating methods of such electrothermal devices were discussed very widely. Some solutions and analytical methods for accurate modeling of such systems were described.

In the chapter some basic sources of numerical analysis errors were discussed and simulation results were compared to analytical description of the problem and experimental data. In spite of many advantages of calculating systems, the accuracy of results should be always taken into account as a basic requirement. Numerical simulation results of magnetic field distribution show a significant differences between analyzed case depended of many factors, such as the manner of assuming power source in inductor, discretization rate or solver used during simulation process. This study has shown the disadvantages of the coupled field modeling with analytical approach. The calculated results of magnetic field intensity and current densities were two times different. The differences reached during the simulation process enable us to affirm the low usefulness of numerical simulation in practical problems and quantitative simulation of induction heating process. According to the experiment, it is also necessary to put more accurate physical properties at different temperatures to describe the behavior of the material correctly.

Most popular methods for accurate power control in induction heating systems were discussed in the case of nonlinearity material properties. Some examples were shown and classical approach for power control in the systems was compared to pulse width modulation case. The advantages and disadvantages of proposed construction and process solutions were discussed. It has been proved that the power system influence is not practically determined in respect of necessity of coupling the field (inductor – workpiece) and the circuit (power supply – load) analysis. Omission of such coupling can provide a very unserviceable results.

9. References

Davies E. J.: Conduction and induction heating, *Peter Peregrinus Ltd.*, London, United Kingdom 1990.

Haimbaugh R., E.: Practical induction heat treating, *ASM International*, 2001.

Rudnev V.: Handbook of induction heating, *Marcel Dekker*, 2003.

Rapoport E., Pleshivtseva Y.: Optimal control of induction heating processes, *CRC/Taylor & Francis*, 2006.

Sajdak C., Samek E.: Nagrzewanie indukcyjne. *Wyd. Śląsk*, Katowice 1985.

UIE: Electromagnetic Induction and Electric Conduction in Industry. Centre Français l'Ėlectricite 1997.

Zgraja J., Bereza J., (2003) "Computer simulation of induction heating system with series inverter", *COMPEL: The International Journal for Computation and Mathematics in Electrical and Electronic Engineering*, Vol. 22 Iss: 1, pp.48 – 57.

Paya B., Fireteanu V., Spahiu A., Guerin C.: 3D Magneto-Thermal Computations in Induction Heating. Models and Experimental Validations, *10th International IGTE Symposium on Numerical Field Calculation in Electrical Engineering*, September 16-18, 2002, Graz, Austria.

Niedbała R.: Charakterystyka energetyczna indukcyjnego nagrzewania objętościowego. *Zeszyty Naukowe Politechniki Łódzkiej „Elektryka"* nr 101, s 107-114, Łódź 2003.

Kainuma K., Sakuma M.: Application of Numerical Analysis to Industrial Electrical Heating *Products*. Fuji Electric Journal 1998, Vol. 71, No.5.

Chaboudez C., Clain S., Glardon R., Rappaz J., Swierkosz M., Touzani R.: Numerical Modelling of Induction Heating of Long Workpieces, *IEEE Treansaction on magnetics*, vol.30, no.6, 1994.

Biro O., Preis K., Richter K., R.: Various FEM formulations for the calculation of transient 3d eddy currents in nonlinear media, *IEEE Treansaction on magnetics*, vol.31, no.3, 1995.

Matthes H., Jürgens R.: 1.6 MW 150 kHz Series Resonant Circuit Converter incorporating IGBT Devices for welding applications. *International Induction Heating Seminar*, 1998 Padova, pp 25-31.

Niedbała R.: Tranzystorowy falownik napięcia zasilający indukcyjny układ grzejny. *Przegląd Elektrotechniczny* 2004, nr 11, s.1149...1152.

Dede J., Jordan J., Esteve V., Ferreres A., Espi J.: On the Behaviour of Series and Parallel Resonant Inverters for Induction Heating under Short-Circuit Conditions. *PCIM Europe 1998 Power Conversion*, pp 301-307.

Nerg J., Partanen J.: Numerical Solution of 2D and 3D Induction Heating Problems with Non Linear Material Properties Taken into Account. *IEEE Transactions on Magnetics*, vol. 36 no.

Galunin S., Zlobina M., Blinov Yu., Nikanorov A., Zedler T., Nacke B., Electrothermal Modeling and Numerical Optimization of Induction System for Disk Heating, *International Scientific Colloquium Modeling for Material Processing.* Riga, 2006.

Niedbała R.: Sterowanie energią elektryczną w procesie indukcyjnego nagrzewania stali. *Przegląd Elektrotechniczny* 2009, nr 6, s.58...62.

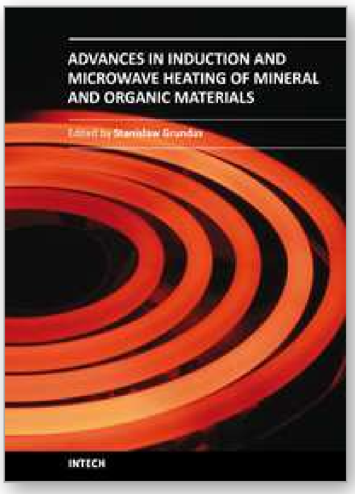

Advances in Induction and Microwave Heating of Mineral and Organic Materials
Edited by Prof. StanisÅ‚aw Grundas

ISBN 978-953-307-522-8
Hard cover, 752 pages
Publisher InTech
Published online 14, February, 2011
Published in print edition February, 2011

The book offers comprehensive coverage of the broad range of scientific knowledge in the fields of advances in induction and microwave heating of mineral and organic materials. Beginning with industry application in many areas of practical application to mineral materials and ending with raw materials of agriculture origin the authors, specialists in different scientific area, present their results in the two sections: Section 1-Induction and Microwave Heating of Mineral Materials, and Section 2-Microwave Heating of Organic Materials.

INTECH
open science | open minds

InTech Europe
University Campus STeP Ri
Slavka Krautzeka 83/A
51000 Rijeka, Croatia
Phone: +385 (51) 770 447
Fax: +385 (51) 686 166
www.intechopen.com

InTech China
Unit 405, Office Block, Hotel Equatorial Shanghai
No.65, Yan An Road (West), Shanghai, 200040, China
中国上海市延安西路65号上海国际贵都大饭店办公楼405单元
Phone: +86-21-62489820
Fax: +86-21-62489821